文章编号：1001-9014(2022)01-0248-05

DOI:10.11972/j.issn.1001-9014.2022.01.018

Tuning the optical response of long-wavelength InAs/GaSb Type-II superlattices infrared focal plane arrays with multi-coatings

SHI Rui[1,2], ZHOU Jian[1], BAI Zhi-Zhong[1], XU Zhi-Cheng[1], ZHOU Yi[1], LIANG Zhao-Ming[1], SHI Ying[1], XU Qing-Qing[1], CHEN Jian-Xin[1*]

(1. Key Laboratory of Infrared Imaging Materials and Devices, Shanghai Institute of Technical Physics, Chinese Academy of Sciences, Shanghai 200083, China;
2. School of Information Science and Technology, Shanghai Tech University, Shanghai 201210, China)

Abstract: In this paper, the multi-coatings composed of layers of zinc sulfide and germanium were designed and fabricated on a long-wavelength InAs/GaSb Type-II superlattices infrared focal plane arrays (FPAs). Compared with the FPAs without multi-coatings, the multi-coatings make the response peaks of the FPAs shift from the wavelength of 8.7 μm and 10.3 μm to that of 9.8 μm and 11.7 μm. The 50% response cut-off wavelength of the FPAs shifts from 11.6 μm to 12.3 μm, and the response intensity of the FPAs is increased by 69% at the wavelength of 12 μm. In summary, the multi-coatings make the response wavelength of the FPAs tunable, which provides a powerful platform for more sensitive long-wave detection and improving imaging capabilities.

Key words: Type-II superlattices, FPAs, multi-coatings, tunable response

基于多层薄膜的长波红外InAs/GaSb II类超晶格焦平面光响应调控研究

史 睿[1,2], 周 建[1], 白治中[1], 徐志成[1], 周 易[1], 梁钊铭[1], 师 瑛[1], 徐庆庆[1], 陈建新[1*]

(1. 中国科学院上海技术物理研究所 红外成像材料与器件重点实验室,上海 200083;
2. 上海科技大学 信息学院,上海 201210)

摘要:本文基于长波InAs / GaSb II类超晶格红外焦平面阵列(Focal Plane Array, FPA)设计和生长了由ZnS和Ge组成的多层薄膜结构。与没有多层薄膜的FPA相比,多层薄膜使其响应峰位置从8.7 μm和10.3 μm分别移动到9.8 μm和11.7 μm, 50%响应截止波长从11.6 μm移动至12.3 μm,并且在波长为12 μm处的响应强度增加了69%。总之,优化的多层薄膜可以调控FPA的响应波长,这为实现更高灵敏度和更高成像能力的长波红外探测提供了更好的平台。

关 键 词:II类超晶格;焦平面阵列;多层薄膜;响应调控

中图分类号:O43;O47　　**文献标识码**:A

Introduction

High-performance long wavelength (LW) infrared photodetectors have important applications in civil and military fields[1-4]. Type II superlattice (T2SL) structure using InAs/GaSb material can cover a wide detection wavelength range from about 1 μm to 30 μm and may have some advantages compared to HgCdTe detectors in terms of uniformity and cost[5, 6]. As we know, T2SL photodetectors possess lower quantum efficiency (QE) than HgCdTe counterparts due to the smaller overlap of the electron-hole wave functions[7]. When the detection

Received date: 2020-06-18, **revised date**: 2020-07-23　　**收稿日期**:2020-06-18,**修回日期**:2020-07-23

Foundation items: Supported by the National Natural Science Foundation of China (NSFC) (61904183, and 61974152), the National Key Research and Development Program of China (2016YFB0402403), the Youth Innovation Promotion Association, CAS (2016219), the Innovation Engineering Frontier Program of SITP, CAS (233) and the Fund of Shanghai Science and Technology Foundation (16JC1400403).

Biography: Shi Rui (1995-), male, Jiuquan Gansu, master. Research area involves Semiconductor materials and devices. E-mail: 1249359402@qq.com; These authors are equal contribution to this work

* **Corresponding author**: E-mail: jianxinchen@mail.sitp.ac.cn

wavelength of T2SL photodetectors increases, the overlap part of the electron-hole wave function is further reduced. One approach to make up this shortcoming is to use anti-reflection coatings. At the same time, the response spectrum is also an important property of long wavelength photo-detector. For a superlattice LWIR detector, its response spectrum is usually modulated by multiple pass reflection within the detector due to the smaller absorption coefficient. In many applications, strengthen the response at some specific wavelength is very necessary, especially the response around the cut-off wavelength. Multi-coatings technology can also be provided to tune the response spectrum of superlattice photodetector. [7-11] However, there are few studies on the combination of infrared detector and multi-coatings, especially on the long-wavelength devices. In this paper, we demonstrate an approach to tune the response of long-wavelength InAs/GaSb Type-II superlattices infrared focal plane arrays with multi-coatings.

1 Design method and proposed structure

The detailed optical behavior of the T2SL infrared photodetectors for each considered wavelength can be solved by applying electromagnetic (EM) theory. The incident plane wave propagates along the z-direction and polarizes with the electric field parallel to the x(TM) and y (TE) direction, respectively. The incident electric field intensity is assumed to be $Ex=E_Y=[1V/m]\exp(-jkz)$. The absorption per unit volume is defined as [12]

$$A(\lambda)=\frac{1}{a^2}\int_s \varepsilon''(\lambda)\left|E(\lambda)\right|^2 \mathrm{d}x\mathrm{d}y\mathrm{d}z\mathrm{d}\lambda,, \qquad (1)$$

where $|E(\lambda)|^2$ is the normalized total intensity, ε'' is the imaginary part of dielectric function of T2SLs, $\mathrm{d}\lambda$ is the wavelength step used in this simulation, and a is the pixel center distance.

In the numerical simulation, the 2D finite element method (FEM) is adopted for the T2SL infrared photodetectors[13]. On one hand, the perfect matched layer (PML) is adopted as the absorbing boundary condition for the analysis of electromagnetic scattering problems. On the other hand, the periodic boundary condition is used between the adjacent pixels. In this work, the pitch width is set to be 30 μm, and the ditch width is 3 μm. The electrode material is Au, the center distance and thickness of it are 16 μm and 500 nm, respectively. The T2SL (14 ML InAs/7 ML GaSb) is designed as intrinsic absorption material, the center distance and thickness of it are 27 μm and 3.5 μm, respectively. All the geometric dimensions set above remain the same situation, unless mentioned otherwise. The InAs/GaSb-based superlattice materials involved in this work were grown on n-type GaSb substrates by solid-source molecular beam epitaxy (MBE). A 320×256 T2SL FPAs with cut-off wavelength of 14 μm were designed and fabricated to explore the tunable spectrum response. Because of the large absorption coefficient of the GaSb substrate at the wavelength of 8~14 μm, it is necessary to remove the epitaxial substrate completely to obtain large response from FPA. In the process of removing substrate, the surface of the GaSb substrate was thinned to 100 μm by polishing machine firstly, and then the epitaxial substrate of GaSb was completely removed by etching solution composed of CrO_3, HF and H_2O with a ratio of 5 g: 5 ml: 500 ml. Zinc sulfide (ZnS) and germanium (Ge) or a combination of them have no or weak absorption in long wavelength infrared radiation. The multi-layer coatings are deposited on the InAsSb buffer surface using physical vapor deposition (PVD) method.

2 Results and discussion

In order to explore the optical properties of focal plane arrays (FPAs) under back illumination, the refractive index of InAsSb should be confirmed firstly. InAsSb, as a buffer layer grown between SLs and the interface of GaSb substrate effects the response spectrum of FPAs. But it is hard to determine because of the heavy doping Si. Here, the response spectrum of single-unit device under front illumination, as shown in the inset of Fig. 2(a), was used to confirm the refractive index of InAsSb. It is clear that the response peaks appear at 8.7 μm and 11.5 μm, respectively. This is due to the large difference in refractive index between Air and SLs, SLs and InAsSb, which excites the Fabry-Perot resonance in

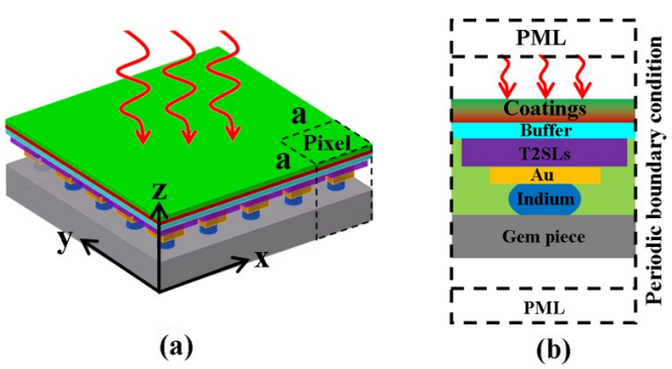

Fig. 1 (a) The 3D schematic diagram and (b) the center cross-section of a pixel with infrared radiation at the normal angle as the simulated and experimental multilayer coatings for T2SL infrared photodetector model in this study
图1 T2SL红外光电探测器与多层薄膜结合的仿真与实验模型(a)3D结构示意图和(b)背入射的中心截面图

the SLs cavity.

To identify the important influence of InAsSb layer, we assume the refractive indices of InAsSb are 1.5, 2, 2.5, and calculate the response spectrum, which is well-agreed with the experiment spectrum when the refractive index equals 2, as shown in Fig. 2(b). It is found that the intensity of response decreases as the refractive index increases, which is due to the refractive index of InAsSb is approaching to that of SLs, leading to the decreasing strength of resonance. It is interesting that the response peak redshifts with increasing the refractive index of InAsSb between 8.5 μm to 9 μm, while the position of response peak does not move with increasing the refractive index of InAsSb at 11.5 μm. Fig. 2(c) shows the optical field distribution when the refractive index of InAsSb is 2 and the response wavelengths are 11.5 μm and 8.7 μm, respectively. It can be found that F-P resonance is excited and most of light is confined to SLs cavity, and the corresponding resonant orders are 2 and 3, respectively.

Firstly, single ZnS layer was designed for the T2SL infrared photodetector and the numerically calculated absorption spectrum as functions of wavelength and the thickness of ZnS, and the results are shown as the color pattern in Fig. 3(a). It is found that the absorption peaks are systematically redshifted and the numbers of absorption peaks increase as a function of increasing thickness of ZnS. In order to identify the cavity resonances corresponding to the absorption peaks, we found that the Fabry-Perot resonances can be excited in the ZnS cavity if the condition is satisfied as[15, 16]

$$2\,n\,dZnS = m\,\lambda \qquad (2)$$

where n and d_{ZnS} are the refractive index and thickness of ZnS, respectively, and m equals 1, 2, 3…etc. The relation between the radiation wavelength and the thickness of ZnS was calculated by using the Equation (2), shown as the color dash curves in Fig. 3(a). It is clearly that the position of the main resonant absorption peaks are well-consistent with that achieved by the calculation (m=1, 2, respectively), allowing a part of infrared radiation light coupling into intrinsic absorption material. As a result, the unfolding absorption peaks are broadened by the main resonance in intrinsic absorption zone which is overlaid with the resonance excited within the ZnS layer. We focus on the responsivity spectrum from 8 μm to 14 μm, which is the atmospheric window. Fig. 3(b) shows the simulation and Fig. 3(c) shows the experimental response spectra of T2SL FPAs without and with the ZnS layer of 0.5 μm thickness, respectively. It is found that a response peak appears around the wavelength of 12.5 μm, which means that the ZnS coating played as an antireflection role. In addition, the ZnS film can perturb the intrinsic resonance mode of the detector and cause a slight blueshift of the absorption peak.

To further study the optical response property by coatings, the FPAs combined with three-layers (ZnS-Ge-ZnS) was designed and fabricated. Similar to the monolayer design method, we calculated the thickness combinations of all ZnS, Ge, and ZnS with a range from 0.1 μm to 2.0 μm and a step size of 0.1 μm. The optimized thicknesses of ZnS, Ge and ZnS films are 0.2, 1.5 and 0.4 μm, respectively, which were chosen from the calculated data. Fig. 4(a) shows the simulation and the experimental response spectra of T2SL FPAs with this designed multi-coatings, and the experimental response spectra are good agreed with that of the simulation data. It is interesting that the two simulation response peaks at 9.8 μm and 12.1 μm are caused by different physical mechanisms in the coupling process of light and matter. The Electrical field distribution indicates that the loss is mainly determined by the specular reflection at 9.8 μm and diffuse transmission at 12.1 μm, as shown the inset of Fig. 4(a). It is found that the full width at half maximum (FWHM) of experimental spectra is wider than that of simulation due to the lower quality factor, which depends not only on the structure of the detector but also the process conditions, such as surface roughness and mesa steepness, and so on. Through the comparison and analysis of the experiment results, the impact of multi-coatings on FPA's response mainly includes two as-

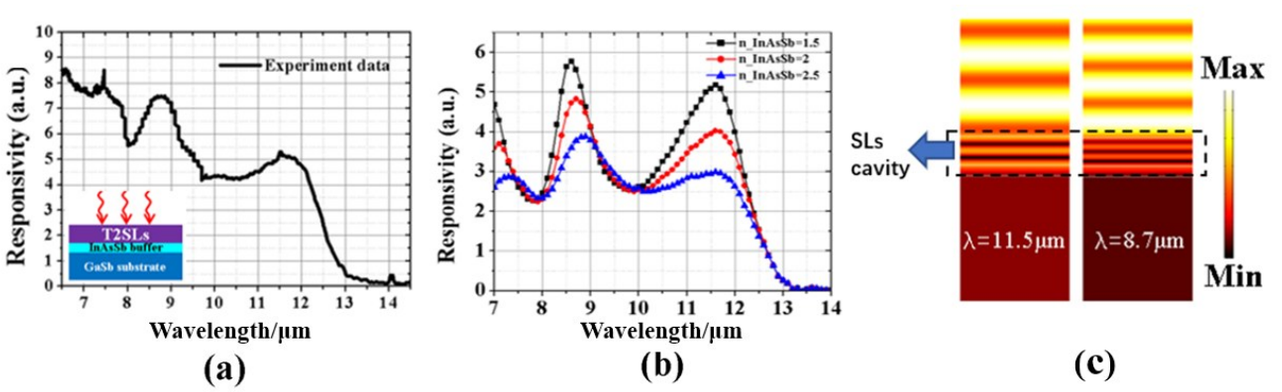

Fig. 2 The response spectra of single-unit device under front illumination, (a) experimental and (b) simulation spectra assuming the refractive indices of InAsSb are 1.5, 2 and 2.5, respectively. (c) the optical field distribution when the refractive index of InAsSb is 2 and the response wavelengths are 11.5 μm and 8.7 μm, respectively

图2 正入射单元器件的响应光谱,(a)实验响应光谱和(b)假设InAsSb的折射率分别为1.5、2和2.5的模拟响应光谱,(c)InAsSb的折射率为2时波长分别为11.5 μm和8.7 μm对应的光场分布

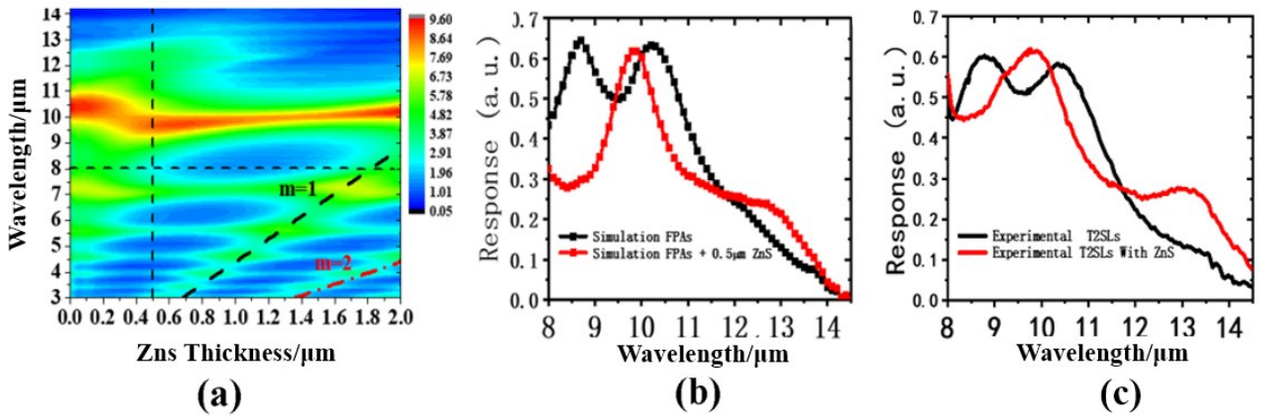

Fig. 3 (a) The T2SLs numerically calculated absorption spectra as functions of the wavelength of incident light and the thickness of ZnS under normal illumination, (b) the simulation and (c) experimental responsivity spectra of T2SLs without and with the thickness of ZnS of 0.5 μm, respectively
图3(a)T2SLs在背入射条件下根据入射光的波长和ZnS的厚度计算的吸收光谱,生长0.5μm的ZnS前后T2SL的(b)仿真响应光谱和(c)实验响应光谱

pects. Firstly, the detector forms an F-P cavity resonance combined with the multi-coating, and resonance affect is excited by the coupling of incident light and FPA, which effects the 50% cut-off wavelength of the device. Secondly, according to the Fresnel reflection principle and Maxwell′s equations, the multi-coatings can also affect the reflection of incident light on the surface of the device, which affects the intensity of the device′s response spectra. However, the enhancement of absorption is not correctly consistent with that of the transmission region. In other words, the combined application of multi-coatings and detector is not a simple linear superposition. Therefore, the global design of complex structure should be considered. Compared with the FPAs without multi-coatings, the multi-coatings shift the response peaks from 8.7 μm and 10.3 μm, respectively, to 9.8 μm and 11.7 μm, and shifts the detector's cut-off wavelength from 11.6 μm to 12.3 μm. The response of FPAs is increased by 69% at the wavelength of 12 μm, as shown in Fig. 4 (b). Therefore, the multi-coatings can strengthen FPA's response to long wavelength signals.

3 Conclusion

In this paper, the multi-coatings composed of layers of ZnS, and Ge was applied to a long-wavelength InAs/GaSb Type-II superlattices FPAs. The multi-coatings make the response peaks of FPAs shift from the wavelengths of 8.7 μm and 10.3 μm to that of 9.8 μm and 11.7 μm in comparison with original FPAs. As a result, the 50% cut-off wavelength of FPAs shifts from 11.6 μm to 12.3 μm, and the response from FPAs is increased by 69% at the wavelength of 12 μm. The multi-coatings make FPAs more sensitive to long wavelength signals and can improve the imaging capabilities. Our next work is to

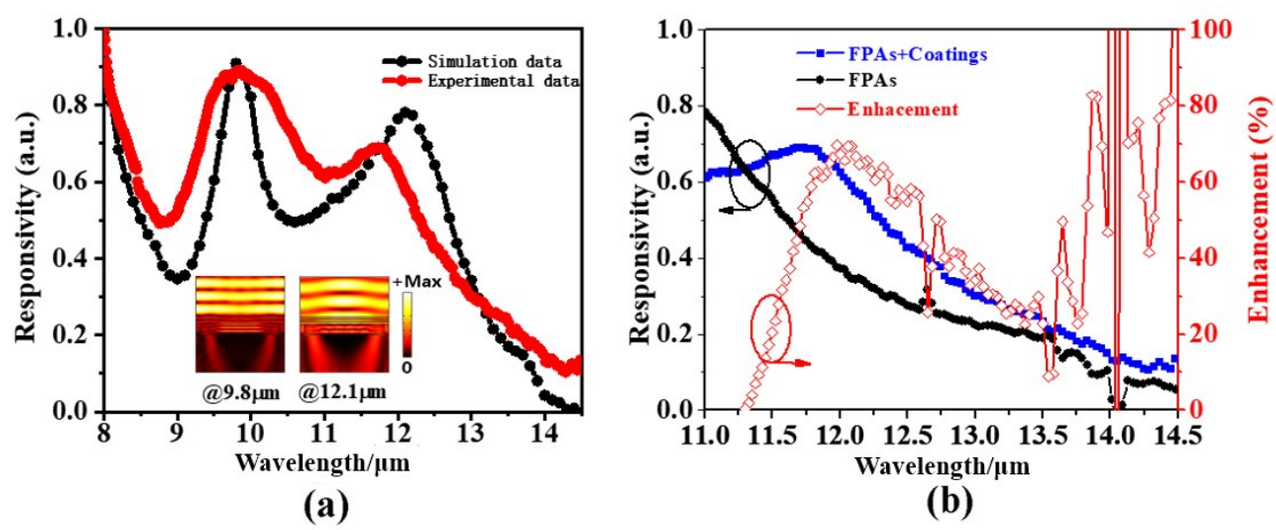

Fig. 4 (a) The simulation and experimental response spectra of T2SL FPAs, (b) the comparison and enhancement of the FPAs' response without and with multi-coatings
图4 (a)T2SL FPAs的仿真和实验响应光谱,(b)FPAs在生长多层薄膜前后响应光谱的比较以及增强幅度

use the multi-coatings to design and realize broadband high quantum efficiency of InAs/GaSb Type-II superlattices long-wave FPAs.

Acknowledgment

This work was supported by the National Natural Science Foundation of China (NSFC) (Grant Nos. 61904183, and 61974152), the National Key Research and Development Program of China (Grant No. 2016YFB0402403), the Youth Innovation Promotion Association, CAS (Grant No. 2016219), the Innovation Engineering Frontier Program of SITP, CAS (CX No. 233) and the Fund of Shanghai Science and Technology Foundation (Grant No. 16JC1400403).

References

[1] Hoang A M, Chen G, Haddadi A, *et al*. Demonstration of high performance bias-selectable dual-band short-/mid-wavelength infrared photodetectors based on type-II InAs/GaSb/AlSb superlattices [J]. *Applied Physics Letters*, 2013, **102**(1): 11108-11130.

[2] CHEN J X, ZHOU Y, XU Z C, *et al*. InAs/GaSb type-Ⅱ superlattice mid-wavelength infrared focal plane array detectors grown by molecular beam epitaxy [J]. *Journal of Crystal Growth*, 2013. **378**: p. 596-599.

[3] Pour S A, HUANG E K, CHEN G, *et al*. High operating temperature midwave infrared photodiodes and focal plane arrays based on type-II InAs/GaSb superlattices [J]. *Applied Physics Letters*, 2011. **98**: p. 143501 - 143501.

[4] Lin P T. Ultra Broadband Mid-IR Detectors Using Multilayer Anti-reflection Coupling [J]. *Optical Society of America*, 2011.

[5] Delaunay P Y, Nguyen B M, Razeghi M. Background limited performance of long-wavelength infrared focal plane arrays fabricated from Type-II InAs/GaSb M-structure superlattice [J]. *Proceedings of SPIE - The International Society for Optical Engineering*, 2009.

[6] SUN Y Y, YANG C A, ZHENG D N, *et al*. Broadband antireflection coating for the near-infrared InAs/GaSb Type-II superlattices photodetectors by lift-off process; proceedings of the Infrared, Millimeter-Wave, and Terahertz Technologies V, F, 2018 [C].

[7] Matsuoka Y, Mathonneire S, Peters S , *et al*. Broadband multilayer anti-reflection coating for mid-infrared range from 7 μm to 12 μm [J]. *Applied Optics*, 2018, **57**(7): 1645-1649.

[8] Sprafke T, Beletic J W. High-Performance Infrared Focal Plane Arrays for Space Applications [J]. *Optics & Photonics News*, 2008, **19**(6): 22-37.

[9] Ciracì C, Urzhumov Y, Smith D R. Far-field analysis of axially symmetric three-dimensional directional cloaks [J]. *Optics Express*, 2013, **21**(8): 9397-9406.

[10] ZHOU J, Zhang Z Y, Wu Y G, *et al*. Significantly enhanced coupling to half-space irradiation using a partially capped nanowire for solar cells [J]. *Nano Energy*, 2018, **45**: p. 61-67.

[11] Kweun J M, Lee H J, Oh J H, *et al*. Transmodal Fabry-Perot Resonance: Theory and Realization with Elastic Metamaterials [J]. *Physical review letters*, 2017, **118**(20): 205901.1-.6.

[12] Shabahang S, Kondakci H E, Villinger M L, *et al*. Omni-resonant optical micro-cavity [J]. *Scientific Reports*, 2017, **7**(1).

[13] Rhier D R. HgCdTe Long-Wave Infrared Detectors [J]. *Semiconductors & Semimetals*, 2011, **84**: 303-331.